Apparent oscillator strengths for molecular oxygen derived from electron energy-loss measurements*

Russell H. Huebner

Argonne National Laboratory, Argonne, Illinois 60439

R. J. Celotta, S. R. Mielczarek, and C. E. Kuyatt

National Bureau of Standards, Washington, D.C. 20234
(Received 8 January 1975)

Oscillator strengths for O_2 from 6 to 14 eV are derived from the energy-loss spectrum of 100 eV incident electrons. Integrated f values for the Schumann–Runge bands and continuum, which span four orders of magnitude in intensity, agree well with high-resolution photoabsorption measurements. Vibrational structure superimposed on the Schumann–Runge continuum, previously assigned to the $(3s\sigma_g)\,^3\Pi_g$ Rydberg state, contributes less than 0.5% to the total oscillator strength determined for that region. These data also yield f values for discrete bands in the region between 9.5 and 14.0 eV, where line saturation problems complicate oscillator strength analysis of the optical data. An oscillator strength sum of 0.198 is obtained for all transitions below the ionization potential at 12.07 eV.

I. INTRODUCTION

Oxygen, the second most abundant molecule in the atmosphere, plays an important role in a variety of combustion and energy conversion processes. In the life sciences it is a key element in respiration. It is also important in atmospheric photochemistry and other phenomena such as aurora and dayglow. Molecular oxygen is also involved in many nuclear radiation problems, for example, in the energy degradation of ionizing radiation in air and in the quenching of radiation-induced luminescence in liquids. Consequently, the microscopic processes of energy absorption by O_2 are of considerable interest not only from a fundamental but also a practical viewpoint.

The spectrum of energy absorption by O_2 has been studied optically by many workers. The results have been critically reviewed by Krupenie[1] and by Hudson.[2] Lassettre and co-workers[3,4] have studied the inelastic scattering of 500 eV electrons from O_2 and used their data to derive oscillator strengths at a number of energy loss values in the O_2 spectrum. However, because the resolution of this early work was comparatively low, oscillator strengths for many unresolved transitions could not be separately determined. In a series of papers[5–8] we have recently reported apparent oscillator strength distributions for a number of molecules derived from high-resolution electron energy-loss spectra. These data have been in generally good agreement with optically measured values. In this paper we present similarly derived values for O_2 for energy losses between 5 and 14 eV.

II. EXPERIMENTAL METHOD AND PROCEDURE

The high-resolution electron energy-loss spectrum (Fig. 1) of O_2 was measured with the NBS model AN-1 electron impact spectrometer[9] for 100 eV electrons scattered within 20 mrad of the incident direction. The energy-loss spectrum was recorded digitally by counting the number of inelastically scattered electrons in 10 meV energy-loss intervals. The count was stored in an on-line computer operated in a multichannel scaling mode. The spectrum was swept between selected energy loss points of 4.50 and 14.09 eV and between 21.00 and 21.39 eV alternately for increasing and decreasing energy loss. This was done so that pressure and electron beam fluctuations would be averaged out. The spectrum shown in Fig. 1 was accumulated for 200 sweeps with a counting time per channel of 17 msec in each sweep.

The data were corrected in two ways. First, the count rate is adjusted to allow for dead time in counting circuitry. Because of the high speed of the counting electronics, the major dead time comes from the pulse length itself. The dead time (τ) of this system was measured to be 20 nsec, and a dead time correction of the form $1/(1-R\tau)$ was applied, where R is the uncorrected count rate. This correction assures linearity of the spectrum over many decades of accumulated count.

The second correction was made to adjust the energy loss scale to a calibrated energy-loss point. For this purpose, comparable parts of helium and oxygen (0.1069 and 0.1599 torr, respectively) were leaked together into the apparatus. Pressures were measured with a capacitance manometer. The energy-loss scale was then adjusted so that the $2\,^1P - 1\,^1S$ transition in helium was positioned at 21.216 eV. Further, a total-system energy resolution of 30 meV was determined from the measured full width at half-maximum for this transition. Research-grade oxygen with a stated purity of 99.99% was used.

An apparent oscillator strength distribution was derived from the energy loss data by a procedure discussed in detail elsewhere.[6] This procedure yields a relative oscillator strength distribution from the energy-loss data by correcting for a finite angular acceptance of the apparatus. The relative distribution is then normalized at one point in the spectrum, preferably in a region of continuous absorption, to a differential oscillator strength determined from optical measure-

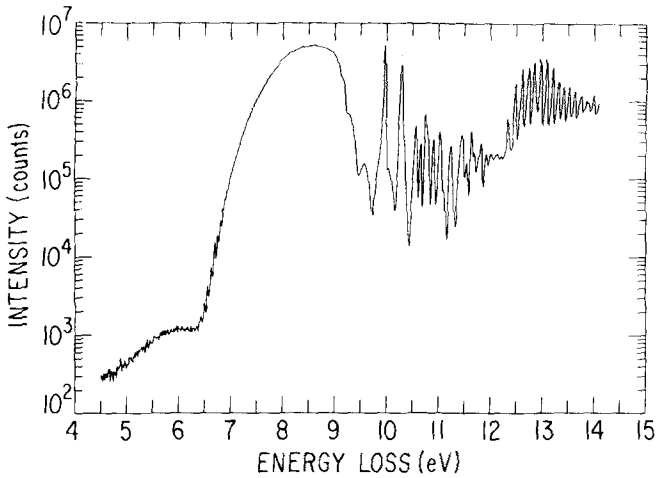

FIG. 1. Electron energy-loss spectrum of molecular oxygen for 100 eV incident electrons scattered at zero angle.

ments. Application of this method for incident energies as low as 100 eV is based on the theory of limiting oscillator strengths developed by Lassettre.[10] That is, for zero momentum transfer the limiting value of the generalized oscillator strength is the optical oscillator strength regardless of whether the Born approximation holds. In practice, this means that the relative oscillator strength distribution determined from energy-loss spectra at small scattering angles (i.e., small momentum transfer) should closely resemble the optical oscillator-strength distribution.

Aside from the above, other qualifications outlined in Ref. 6 have prompted use of the term "apparent" in describing oscillator strength distributions derived by this procedure. One qualification concerns neglect of higher order terms in the expansion of the generalized oscillator strength $f(K)$, where $\hbar K$ is the momentum transfer. This is likely to produce deviations from the optical distribution, particularly when the shape of the generalized oscillator strength at small $\hbar K$ changes significantly for different energy losses. For O_2, however, measurements[3,4] show that for energy losses below 15 eV the shapes of $f(K)$ are similar.

The apparent oscillator-strength distribution for O_2 was derived from the data in Fig. 1 by use of Eq. (9) of Ref. 6 for an incident energy $T = 100$ eV and maximum acceptance angle $\theta = 0.020$ rad. The data were normalized at 8.61 eV (1440 Å) to an average optical value of $0.135\ \text{eV}^{-1}$ [$\sigma(h\nu) = 1.48 \times 10^{-17}\ \text{cm}^2$] where the photoabsorption measurements of a number of workers appear to be in best agreement (see Fig. 13 of Ref. 2). Figure 2 shows the apparent oscillator strength distribution for O_2 derived in this manner. The total oscillator strength for a particular band located between energies E_1 and E_2 may be obtained from the data of Fig. 2 by integration:

$$f = \int_{E_1}^{E_2} (df/dE)\, dE \quad .$$

We also obtained energy-loss spectra for 300 eV incident electrons on O_2, although the data were of generally poorer quality. A check of oscillator strengths derived in the same manner from these data showed agreement to about ± 5% over the same energy-loss region.

III. RESULTS

A. The Schumann-Runge bands and continuum region

The intense continuous absorption band with a broad maximum at 8.6 eV (Fig. 2) is the well known Schumann–Runge continuum $B\,^3\Sigma_u^- - X\,^3\Sigma_g^-$. Our values in this region are compared with the data of Watanabe *et al.*[11] in a logarithmic plot in Fig. 3(a). In Fig. 3(b) the same region is compared on a linear scale with a representative selection of optical data.[11–14] The agreement between the optical and electron-impact values is extremely good. Our values agree most closely with the data of Watanabe *et al.*[11] from 7.0 to about 9.7 eV except for a small region between 8.75 and 9.00 eV (1420 to 1380 Å), where their values are about 10% lower. However, as can be seen in Fig. 3(b), other optical values lie above or very near the electron-impact values in this interval. The low-intensity peaks in the spectrum [Fig. 3(a)] below 7.08 eV are the discrete Schumann–Runge bands. On the high-energy side of the continuum two shoulders are observed (Fig. 3) at approximately 9.15 and 9.27 eV along with a broad maximum at 9.58 eV in agreement with the data of Watanabe *et al.*[11] Interpretations of these continua are reviewed by Krupenie[1] and Hudson.[2]

Our energy-loss data in the region of the maximum in the Schumann–Runge continuum are shown in more detail in Fig. 4. The peaks indicated below the spectrum were obtained by subtracting the estimated contribution of the underlying continuum (i.e., indicated by the dashed line) from the measured spectrum. These peaks are not generally apparent in the optical measurements, although such weak structure in a region of intense absorption might easily have been missed by workers using discrete-line sources.[15] However, there is some indication of structure in this region in the energy-loss spectrum of Geiger and Schröder[16] for 25 keV incident electrons. The energy-loss data of Lassettre *et al.*[17] for incident energies of 50 and 70 eV also indicate some structure. Recently, Cartwright *et al.*[18] resolved these

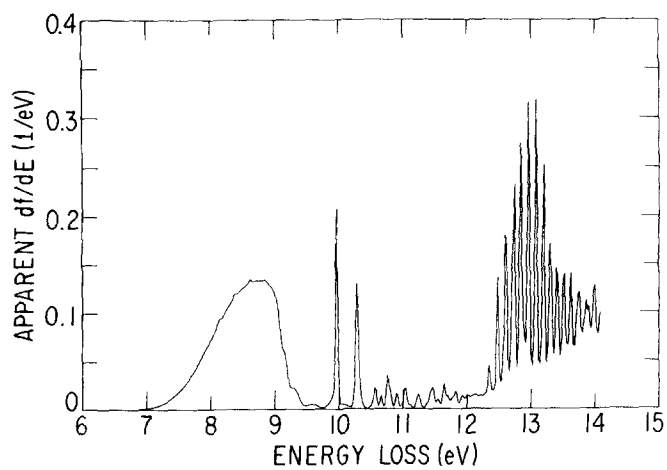

FIG. 2. Apparent oscillator strength distribution for O_2 derived from the energy-loss data of Fig. 1.

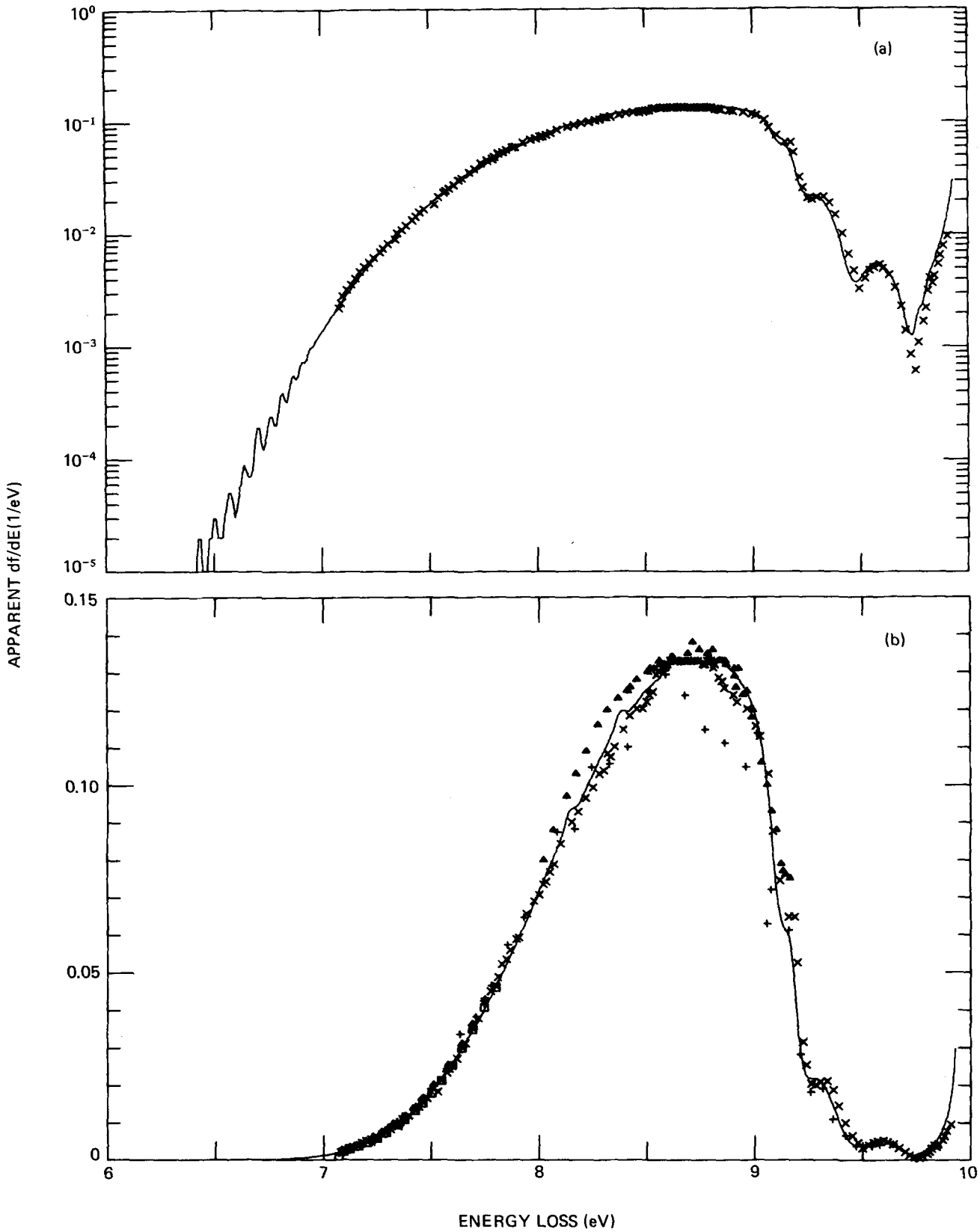

FIG. 3. Comparison of oscillator strengths in the Schumann-Runge region of O_2: (a) logarithmic plot of electron impact results (solid line) with optical data of Ref. 11 (X); (b) linear plot of electron impact results (solid line) with optical data (X—Ref. 11, square—Ref. 12, triangle—Ref. 13, and cross—Ref. 14).

features in the energy-loss spectra for 45 eV incident electrons. They identify these energy losses as due to transitions to the $(3s\sigma_g)^3\Pi_g$ Rydberg state of O_2. This identification is made by comparison with energies of

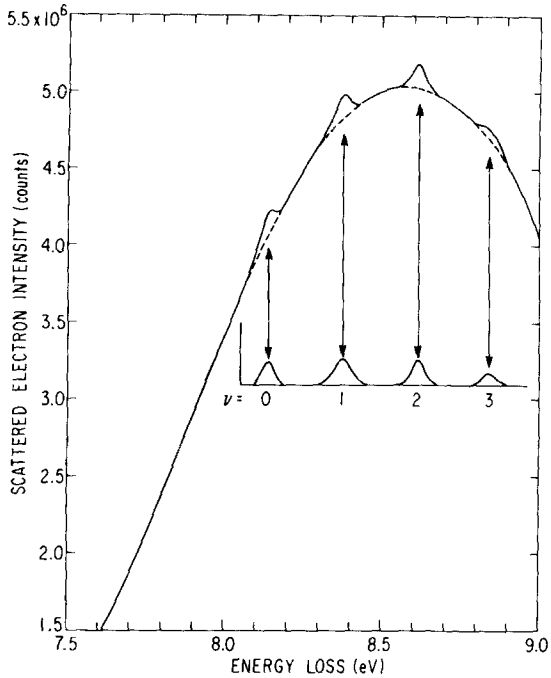

FIG. 4. Energy-loss spectrum of the Schumann–Runge continuum showing discrete structure. Subtraction of estimated continuum contribution (dashed line) from the spectrum yields the peaks indicated below the curve.

the Rydberg states calculated by an improved virtual-orbital method. They also found the dependence on scattering angle to be consistent with that expected for a symmetry-forbidden transition. In Table I the peak energies and intensities are compared with the data of Cartwright *et al.*[18] Our data confirm their observation of the large energy spacing between $v' = 1$ and 2, similar to that found for $O_2^-(^2\Pi_g)$ by Sanche and Schulz.[19] In Table I we also list the apparent oscillator strength for each vibrational member after subtraction of the underlying continuum. It is unclear whether these values should be regarded as "dipole" oscillator strengths, inasmuch as the assignment of this transition as $(3s\sigma_g)^3\Pi_g - X^3\Sigma_g^-$ implies a zero dipole oscillator strength. On the other hand, evidence from both photoabsorption[15] and high-energy electron energy-loss[16] measurements

TABLE I. Comparison of the energies and intensities measured for the $^3\Pi_g$ Rydberg state of oxygen

v'	Energy (eV)	Spacing (eV)	Rel. Intensity	Apparent f value	Ref.
0	8.138 ± 0.010		0.71	18.2×10^{-5}	a
	8.145 ± 0.020		0.73		b
		0.234			a
		0.222			b
1	8.372 ± 0.010		1.00	25.6×10^{-5}	a
	8.366 ± 0.020		1.00		b
		0.242			a
		0.244			b
2	8.614 ± 0.010		0.75	20.8×10^{-5}	a
	8.610 ± 0.020		0.80		b
		0.226			a
		0.215			b
3	8.840 ± 0.010		0.32	9.6×10^{-5}	a
	8.825 ± 0.020		0.25		b
				$\sum_{v'} f_{v'0} = 74.2\times10^{-5}$	

[a]Present work. [b]Reference 18.

TABLE II. Values of f_{cont} for the Schumann–Runge continuum.

	Watanabe, Inn, and Zelikoff[11]	Metzger and Cook[20]	Goldstein and Mastrup[14]
E_1(eV)	7.067	7.079	7.048
E_2(eV)	9.670	9.187	9.744
f(optical)	0.161	0.142	0.156
f(electron impact)	0.162	0.156	0.162

suggests that this transition may have some dipole-allowed character. However, it is also possible that the observed transition probability for this state may arise through quadrupole or magnetic dipole terms. The sum of the apparent oscillator strengths over the four vibrational members yields a value of 7.42×10^{-4}.

In order to obtain a total oscillator strength for the Schumann–Runge continuum one must integrate from the dissociation limit of 7.082 eV to some upper energy cutoff. The choice of this upper energy limit is somewhat complicated by the presence of weak continua in this region, as mentioned earlier. Integration of optical data also encounters this problem and the choice of integration limits by various workers has not always been the same. In Table II we compare f_{cont} values we obtain from the present work with optical values, where the limits of integration were chosen to be the same. These agree to better than 10%, which represents the uncertainty in the normalization value used. Further justification of the specific normalization we have chosen is evident from the consistency of our values with independent measurements made for other spectral features. Rather than the limits of integration shown in Table II we prefer the limits $E_1 = 7.082$ eV and $E_2 = 9.480$ eV, which do not include contribution from the broad maximum near 9.58 eV. This choice yields $f_{cont} = 0.161$. This includes the small contribution (0.46%) from the four peaks superimposed near the maximum of the continuum, as well as an estimated contribution of less than 3% from the weak continua at 9.15 and 9.27 eV.

At the low-energy end of the Schumann–Runge continuum a series of closely spaced peaks are resolved in the energy-loss spectrum (Fig. 1). These are the Schumann–Runge bands converging to the dissociation limit. These peaks are approximately three orders of magnitude less intense than the maximum counting rate in the continuum. We have determined the apparent oscillator strength of each vibrational member of this series by integrating over an energy interval for each peak equal to the band origin separations tabulated by Krupenie.[1] The intervals of integration extend 10 meV above each band origin. This choice positioned the limits of integration very near the minima observed between successive peaks for the vibrational members between $v' = 3$ and $v' = 14$. The limits of integration were then simply extended into the regions where distinct peaks were no longer resolved. A correction was made for each energy interval to subtract out an assumed constant background. This correction contributes a large uncertainty ($\pm 7\times10^{-7}$) to the oscillator strengths determined for bands with $v' < 6$ but has negligible influence for the high-

TABLE III. Oscillator strengths of the Schumann–Runge bands of O_2.

$v'-v$	Band origin (eV)	Optical values					
		Bethke	Halmann	Farmer *et al.*	Ackerman *et al.*	Hasson *et al.*	Electron values
0–0	6.121				3.45×10^{-10}	3.3×10^{-10}	
1–0	6.204				3.9×10^{-9}	3.5×10^{-9}	2.7×10^{-8}
2–0	6.287	2.3×10^{-8}	2.6×10^{-8}	2.69×10^{-8}	2.38×10^{-8}	1.99×10^{-8}	6.2×10^{-8}
3–0	6.366	7.4×10^{-8}	8.2×10^{-8}	1.54×10^{-7}	9.9×10^{-8}	6.8×10^{-8}	5.6×10^{-8}
4–0	6.443	2.74×10^{-7}	2.4×10^{-7}	7.11×10^{-7}	3.21×10^{-7}		2.97×10^{-7}
5–0	6.516	7.28×10^{-7}	7.48×10^{-7}	2.80×10^{-6}	8.52×10^{-7}		7.39×10^{-7}
6–0	6.586	1.73×10^{-6}	1.77×10^{-6}	4.40×10^{-6}	1.91×10^{-6}		1.70×10^{-6}
7–0	6.652	3.56×10^{-6}	4.24×10^{-6}	8.15×10^{-6}	3.81×10^{-6}		3.50×10^{-6}
8–0	6.714	6.75×10^{-6}	6.59×10^{-6}	1.22×10^{-5}	6.68×10^{-6}		6.85×10^{-6} [a]
9–0	6.772	1.07×10^{-5}	1.13×10^{-5}	1.50×10^{-5}	1.06×10^{-5}		1.05×10^{-5}
10–0	6.825	1.56×10^{-5}	1.42×10^{-5}	2.05×10^{-5}	1.57×10^{-5}		1.60×10^{-5}
11–0	6.873	2.16×10^{-5}		2.74×10^{-5}	2.09×10^{-5}		2.26×10^{-5}
12–0	6.916	2.81×10^{-5}		3.58×10^{-5}	2.53×10^{-5}		2.88×10^{-5}
13–0	6.953	3.17×10^{-5}		3.66×10^{-5}	2.88×10^{-5}		3.41×10^{-5}
14–0	6.985	3.24×10^{-5}		3.69×10^{-5}	3.03×10^{-5}		3.77×10^{-5}
15–0	7.011	3.26×10^{-5}		3.77×10^{-5}	2.92×10^{-5}		3.73×10^{-5}
16–0	7.032	3.16×10^{-5}		3.31×10^{-5}	2.59×10^{-5}		3.53×10^{-5}
17–0	7.048	2.94×10^{-5}		3.16×10^{-5}	2.23×10^{-5}		3.03×10^{-5}
18–0	7.061			2.03×10^{-5}	1.83×10^{-5}		2.72×10^{-5}
19–0	7.070			1.74×10^{-5}	1.44×10^{-5}		1.98×10^{-5}
20–0	7.077			1.35×10^{-5}			1.64×10^{-5}

[a] A 10% correction to the 8–0 band was made to account for an estimated contamination of less than 1 ppm of mercury vapor from the diffusion pumps.

er bands.

Oscillator strengths for the Schumann–Runge bands are presented in Table III with optically determined values[21–25] for comparison. The electron impact values agree closely with the optical data of Bethke,[21] Halmann,[22] and Ackerman *et al.*[23] between $v'=4$ and $v'=11$ and approach the higher values of Farmer *et al.*[24] for vibrational members greater than $v'=13$. The trend of the oscillator strengths and vibrational quantum number of the upper state is clearly shown in Fig. 5. The band intensities observed in this work are in better agreement with the data of Bethke[21] than with the relative intensities observed for high-energy electron impact.[16] Within experimental accuracies there is no significant departure from the general trend of the optical data. The present work yields an oscillator strength sum of 32.9×10^{-5} for the Schumann–Runge bands in good agreement with optical values of 25.5×10^{-5}, 31.4×10^{-5}, and 35.4×10^{-5} obtained, respectively, by Ackerman *et al.*,[23] Bethke,[21] and Farmer *et al.*[24]

The band oscillator strengths, $f(v',o)$, are related to the Franck–Condon factors, $q(v',o)$, and to the electronic absorption oscillator strength f_{el} by the expression[21]

$$f(v',o)=f_{el}q(v',o)E(v',o)/E_m \ ,$$

where $E(v',o)$ is the energy of the band origin, and E_m is the weighted average energy of the transition (i.e., a value $E_m=8.53$ eV divides equally the total oscillator strength of the Schumann–Runge region). Recently, Albritton[26] has calculated precisely the Franck–Condon factors for the $B\,^3\Sigma_u^-(v')-X\,^3\Sigma_g^-(v''=o)$ transition for $v'=4$ through 13. His calculations are based on a RKR potential derived from the most accurate spectroscopic data available and are considered to be highly reliable. Combining these with our data from Table III, we find values of f_{el} from 0.128 to 0.155 with an average of 0.140. These are somewhat smaller than the total f value of 0.162 obtained by integration of our data over the Schumann–Runge bands and continuum. This difference may be accounted for by a falloff in the electronic transition moment at large internuclear separations (i.e., breakdown in the Born–Oppenheimer approximation). However, it is also possible that transitions to another dissociative state (or states) overlapping

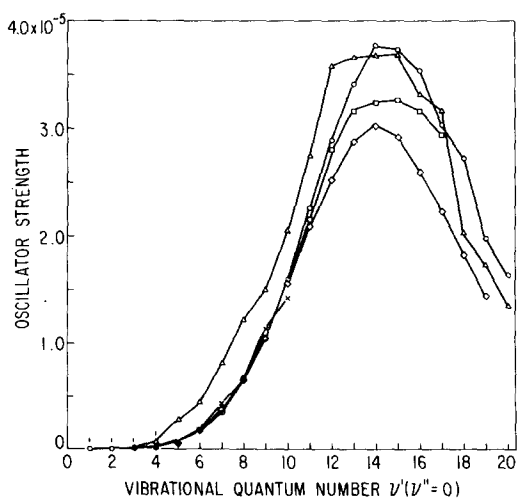

FIG. 5. Comparison of discrete oscillator-strength values for the Schumann-Runge bands: circle—present results; square—Ref. 21; X—Ref. 22; diamond—Ref. 23; triangle—Ref. 24.

the $B\,^3\Sigma_u^-$ state contribute intensity in the Schumann–Runge region.

B. The 9-14 eV energy absorption region of O_2

The region above the Schumann–Runge continuum is complex with discrete absorption. Many high-resolution optical studies have been carried out in this region, and numerous bands, many still unclassified, have been observed.[1,2] In addition to the optical data electron energy loss studies[4,5,16–18] have also been carried out in this region. However, only the data of Lassettre and co-workers[4,5] have been used to provide quantitative estimates of oscillator strengths.

In this region of sharp structure it is difficult to compare directly the photoabsorption data with the present results. This is because of a large difference in the energy resolution achieved in the two techniques. High-resolution optical measurements show higher peaks, deeper valleys, and much narrower peak widths than the comparatively low-resolution electron energy-loss data. This is demonstrated in Fig. 6, where the present data are compared with a summary of optical measurements of Watanabe and co-workers.[27] Other photoabsorption spectra[28–30] show the same behavior. In a spectral region dominated by continuous absorption, this difference vanishes. See Fig. 6, for example, just above the ionization potential (12.07 eV), where the electron and optical values merge.

However, it is precisely the sharpness of the O_2 absorption lines that complicates the determination of f values for discrete bands from the photoabsorption data. Because photon absorption is a resonant process, the measured absorption will depend on both the finite spectral band width of the incident radiation and the natural absorption width of the specific transition, which may vary from one absorption line to another. Thus the measured absorption cross section will exhibit a bandwidth dependence if the natural line width is narrower than the instrumental bandwidth (see Ref. 2 for a more complete discussion). All available photoabsorption cross sections for O_2 in this spectral region are subject to this bandwidth dependence.[2] At an incident energy of 100 eV inelastic electron scattering is a nonresonant process, and experimental difficulties of this kind are absent.

We have determined integrated values of the oscillator strength for small energy-loss intervals in the 9 to 15 eV region. At present there is no other reliable tabulation of f values for transitions in this region. We have chosen energy-loss intervals that separate major features of the spectrum. These correspond closely to the groupings indicated by Tanaka.[31] The f values for these intervals unavoidably include contributions from several unresolved transitions, and no attempt was made to separate them or to subtract any possible underlying continuum. The f values we obtain are listed in Table IV, where the energy intervals are indicated by end points E_1 and E_2. The first column labeled E_m gives the peak energy of the major feature observed between E_1 and E_2. These peak energies agree within ± 0.010 eV with the energies tabulated by Geiger and Schröder[16] for the principal features of their energy-loss spectrum. The last column of the table lists the identification label or upper state designation commonly associated[31,32] with the prominent features in that interval. For more recent attempts at assignments in this region see Cartwright *et al.*[18] and Lindholm.[33]

Besides the general comparison between the present oscillator strength distribution and the optical data (Fig. 6), one additional comparison can be made. Silverman and Lassettre[4] obtained limiting oscillator strength

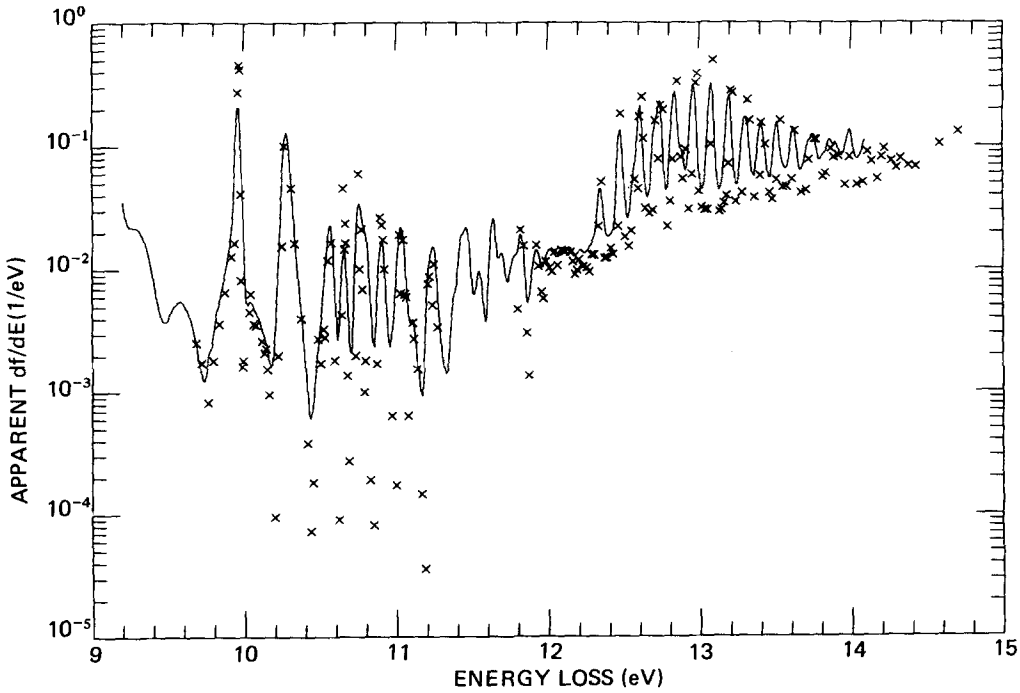

FIG. 6. Comparison of oscillator strengths in the 9–15 eV region of O_2: electron-impact results (solid line); optical values of Ref. 27(X).

TABLE IV. Oscillator strengths for transitions in O_2 from 9.58 to 14.04 eV.

E_m(eV)	E_1(eV)	E_2(eV)	f value	Identification[a]
9.58	9.48	9.74	1.01×10^{-3}	
9.96	9.74	10.18	10.24×10^{-3}	longest band
10.28	10.18	10.44	8.04×10^{-3}	second band
10.57	10.44	10.62	1.47×10^{-3}	third band
10.66	10.62	10.71	6.50×10^{-4}	*a*
10.76	10.71	10.86	2.42×10^{-3}	*a*
10.90	10.86	10.96	9.00×10^{-4}	*b*
11.03	10.96	11.17	1.59×10^{-3}	*b*,*c*
11.24	11.17	11.33	1.10×10^{-3}	*c*
11.46	11.33	11.52	2.10×10^{-3}	*d*
11.55	11.52	11.59	5.02×10^{-4}	(?)
11.64	11.59	11.74	2.05×10^{-3}	*d*
11.82	11.74	11.87	1.63×10^{-3}	*d*
many	11.87	12.10	2.83×10^{-3}	
many	12.10	12.24	1.82×10^{-3}	
12.34	12.24	12.40	3.79×10^{-3}	*H*
12.48	12.40	12.53	7.25×10^{-3}	*H*
12.61	12.53	12.66	11.76×10^{-3}	*H*,*H'*
12.74	12.66	12.78	14.83×10^{-3}	*H*,*H'*
12.84	12.78	12.91	17.24×10^{-3}	*H'*
12.96	12.91	13.02	16.41×10^{-3}	*M*,*H'*
13.08	13.02	13.13	15.67×10^{-3}	*M*
13.20	13.13	13.25	13.90×10^{-3}	*M*
13.30	13.25	13.36	11.86×10^{-3}	*M*,*M'*
13.41	13.36	13.46	9.87×10^{-3}	*M*,*M'*
13.51	13.46	13.57	10.33×10^{-3}	*M'*
13.62	13.57	13.67	9.52×10^{-3}	*M'*
13.75	13.67	13.79	11.66×10^{-3}	*M'*,(?)
13.86	13.79	13.94	14.24×10^{-3}	*J*
13.99	13.94	14.04	10.27×10^{-3}	*J*

[a]See Refs. 31 and 32.

values for energy losses at 9.9 and 12.9 eV by extrapolation of their measurements of the generalized oscillator strength to zero momentum transfer. These values have recently been revised by Lassettre and Skerbele[34] to correct for the streaming error in the McLeod gauge used for pressure measurements in the earlier work. The corrected f values for the peak at 9.9 eV and the region at 12.9 eV (10.8–13.7 eV) are 0.020 and 0.147, respectively. Their 9.9 eV peak observed at low resolution undoubtedly is a composite of the three regions of Table IV, including the longest, second and third bands at 9.96, 10.28, and 10.57 eV. The sum of f values we obtain in the region from 9.74 to 10.66 eV is 0.0198 in excellent agreement. The sum of f values we obtain in the region from 10.71 to 13.67 eV, which spans most of the values presented in Table IV, is 0.159, approximately 8% larger than their result. Similarly, they obtain an oscillator strength of 0.179 for the Schumann–Runge continuum, which is 11% larger than our value of 0.162 for the Schumann–Runge bands and continuum. From this comparison, we conservatively estimate the accuracy of the oscillator strengths obtained in this work to be better than ± 15%.

The present data yield an oscillator strength sum of 0.198 for all transitions below the ionization potential of O_2 at 12.07 eV and of 0.383 below 14.09 eV.

IV. SUMMARY AND CONCLUSIONS

The apparent oscillator strength distribution for O_2 derived in this work agrees well with optical measurements throughout the region investigated. For the first time integrated oscillator strengths for the Schumann–Runge band system have been obtained from electron energy-loss measurements. These values exhibit a dependence on vibrational quantum number of the upper ($^3\Sigma_u^-$) state consistent with high-resolution optical data. Our analysis shows that the same Franck–Condon factors hold for 100 eV incident electrons as for excitation of this transition by photons.

Oscillator strengths were also determined for transitions between 9.5 and 14.09 eV, where optical measurements are complicated by absorption line saturation problems. The close agreement we obtain with the independent measurements of Lassettre and co-workers demonstrate the reliability of the present results. Our tabulation of f values should be a helpful guide for future theoretical assignments of the many unclassified transitions of O_2 below 14 eV.

ACKNOWLEDGMENTS

We thank J. C. Person and M. Inokuti for helpful comments during the preparation of this manuscript and T. Kotek and J. Rundo for the use of their computer plotting program at ANL.

*Work performed in part under the auspices of the U. S. Atomic Energy Commission.

[1]P. H. Krupenie, J. Phys. Chem. Ref. Data 1, 423 (1972).
[2]R. D. Hudson, Rev. Geophys. Space Phys. 9, 305 (1971).
[3]E. N. Lassettre, S. M. Silverman, and M. E. Krasnow, J. Chem. Phys. 40, 1261 (1964).
[4]S. M. Silverman and E. N. Lassettre, J. Chem. Phys. 40, 2922 (1964).
[5]R. H. Huebner, S. R. Mielczarek, and C. E. Kuyatt, Chem. Phys. Lett. 16, 464 (1972).
[6]R. H. Huebner, R. J. Celotta, S. R. Mielczarek, and C. E. Kuyatt, J. Chem. Phys. 59, 5434 (1973).
[7]R. H. Huebner, R. J. Celotta, S. R. Mielczarek, and C. E. Kuyatt, in *Electronic and Atomic Collisions, Abstracts of Papers*. VIII ICPEAC, edited by B. C. Cobic and M. V. Kurepa (Institute of Physics, Beograd, Yugoslovia, 1973), Vol. 1, p. 435.
[8]R. H. Huebner, C. H. Fergurson, R. J. Celotta, and S. R. Mielczarek, in the Proceedings of the IV International Conference on Vacuum Ultraviolet Radiation Physics, Hamburg, Germany, 1974 (Vieweg-Pergamon, to be published).
[9]J. A. Simpson, in *Record of the Tenth Symposium on Electron, Ion, and Laser Beam Technology*, edited by L. Marton (San Francisco Press, San Francisco, 1969), p. 345.
[10]E. N. Lassettre, A. Skerbele, and M. A. Dillon, J. Chem. Phys. 50, 1829 (1969).
[11]K. Watanabe, E. C. Y. Inn, and M. Zelikoff, J. Chem. Phys. 21, 1026 (1953).
[12]R. D. Hudson, V. L. Carter, and J. A. Stein, J. Geophys. Res. 71, 2295 (1966).
[13]A. J. Blake, J. H. Carver, and G. N. Haddad, J. Quant. Spectrosc. Radiat. Transfer 6, 451 (1966).
[14]R. Goldstein and F. N. Mastrup, J. Opt. Soc. Am. 56, 765 (1966).
[15]Structure has been observed in the Schumann–Runge continuum region in photoabsorption studies using continuum light

socurces. See Ref. 14 and M. Bixon, B. Raz, and J. Jortner, Mol. Phys. **17**, 593 (1969).
[16]J. Geiger and B. Schröder, J. Chem. Phys. **49**, 740 (1968).
[17]E. N. Lassettre, A. Skerbele, M. A. Dillon, and K. J. Ross, J. Chem. Phys. **48**, 5066 (1968).
[18]D. C. Cartwright, W. J. Hunt, W. Williams, S. Trajmar, and W. A. Goddard III, Phys. Rev. A **8**, 2436 (1973).
[19]L. Sanche and G. J. Schulz, Phys. Rev. A **6**, 69 (1972).
[20]P. H. Metzger and G. R. Cook, J. Quant. Spectrosc. Radiat. Transfer **4**, 107 (1964).
[21]G. W. Bethke, J. Chem. Phys. **31**, 669 (1959).
[22]M. Halmann, J. Chem. Phys. **44**, 2406 (1966).
[23]M. Ackerman, F. Biaume, and G. Kockarts, Planet. Space Sci. **18**, 1639 (1970).
[24]A. J. D. Farmer, W. Fabian, B. R. Lewis, K. H. Lokan, and G. N. Haddad, J. Quant. Spectrosc. Radiat. Transfer **8**, 1739 (1968).
[25]V. Hasson, G. R. Hebert, and R. W. Nicholls, J. Phys. B **3**, 1188 (1970).
[26]Details of the calculations carried out by Albritton are as yet unpublished, although a tabulation of his results for the Schumann–Runge band system is included in the Krupenie review (Ref. 1).
[27]K. Watanabe, Adv. Geophys. **2**, 153 (1958).
[28]N. Wainfan, W. C. Walker, and G. L. Weissler, Phys. Rev. **99**, 542 (1955).
[29]R. E. Huffman, J. C. Larrabee, and Y. Tanaka, J. Chem. Phys. **40**, 356 (1964).
[30]F. M. Matsunaga and K. Watanabe, Sci. Light **16**, 31 (1967); **16**, 191 (1967).
[31]Y. Tanaka, J. Chem. Phys. **20**, 1728 (1952).
[32]W. C. Price and G. Collins, Phys. Rev. **48**, 714 (1935).
[33]E. Lindholm, Ark. Fys. **40**, 117 (1969).
[34]E. N. Lassettre and A. Skerbele, in *Methods of Experimental Physics, Vol. 3, Molecular Physics, Part B*, edited by D. Williams (Academic, New York, 1973), p. 915.